# Coherent transfer of singlet-triplet qubit states in a scalable architecture of linear quantum dots

Chang Jian Kwong,[1] Teck Seng Koh,[2] and Leong Chuan Kwek[1,3,4,5]

[1] *Centre for Quantum Technologies, National University of Singapore, 3 Science Drive 2, Singapore 117543, Singapore.*
[2] *Ministry of Education, 1 North Buona Vista Drive, Singapore 138675, Singapore.*
[3] *Institute of Advanced Studies, Nanyang Technological University, 60 Nanyang View, Singapore 639673, Singapore.*
[4] *National Institute of Education, Nanyang Technological University, 1 Nanyang Walk, Singapore 637616, Singapore.*
[5] *MajuLab, CNRS-UNS-NUS-NTU International Joint Research Unit, UMI 3654, Singapore.*

arXiv:1602.08596v1 [quant-ph] 27 Feb 2016

We propose two schemes to coherently transfer arbitrary quantum states of the two electron singlet-triplet qubit across an empty chain of quantum dots. The schemes are based on electrical control over the detuning energy of the quantum dots. The first scheme is a pulse-gating scheme, requiring dc pulses and engineering of inter- and intra-dot Coulomb energies. The second scheme is based on the adiabatic theorem, requiring time-dependent linear control of the detuning energy through avoided crossings at a rate that the system remains in the ground state. We simulate the transfer fidelity for 3 dots using typical experimental parameters for silicon quantum dots, then generalize our results to arbitrary number of dots. Our results give state transfer fidelities in excess of 98.7% and 99.3%, and at sub-nanosecond and tens of nanosecond timescales, for the pulse-gated and adiabatic schemes, respectively.

Spin qubits in semiconductor quantum dots are leading candidates for quantum information processing due to their long coherence times [1, 2] and promise of scalability [3]. The exchange coupling is the spin-dependent part of the Coulomb interaction between electrons, and is essential in the manipulation of qubit-qubit interaction [3], as well as single-qubit rotations for qubits encoded by two [4, 5] or three [6, 7] electron spins.

Because of the architectural and scaling constraints [8] imposed by the short range of the exchange interaction [9], studies of spin qubit architectures invariably involve how quantum information may be transferred from one location to another with high fidelity and experimentally realistic requirements. Existing proposals may be based on moving the electrons themselves [10], or utilize exchange-coupled spin chains that require precise engineering of the exchange interaction [11], strong couplings within a "spin bus" [12], or pulse shaping of the tunnel couplings for the single spin qubit [13] and the triple spin qubit [14]. Other proposals based on hybrid systems that transduce spin information into photon modes via a resonant cavity [15–17] introduce new experimental constraints and may be more challenging to realize.

Despite the successes of the two electron singlet-triplet (ST) qubit [2, 18–22], relatively little attention has been given to elucidate techniques for the transfer of quantum information encoded by the ST qubit without posing additional experimental challenges.

In this Letter, we study the coherent transfer of quantum information encoded in the singlet ($S$) and unpolarized triplet ($T_0$) states of the ST qubit across an empty chain of quantum dots, as sketched in Fig. 1(a). We investigate the rate and fidelity of the transfer for two schemes that are within reach of current experimental techniques, requiring only control over the detuning energy $\varepsilon$ of individual quantum dots (Fig. 1(b)).

Our schemes are viable to quantum dots in Si [23] because Si due to its small spin-orbit interaction [24], and low proportion of spinful nuclei (5% of spin-1/2 $^{29}$Si), and can be further isotopically purified. With typical experimental parameters, we find that fidelities higher than 98.7% can be achieved with both schemes. In order to do better than classical communication, the fidelity of state transfer needs to be greater than 2/3 [25], a benchmark our schemes far exceed.

*Theoretical Model.*– We consider a linear chain of $N$ quantum dots with nearest neighbour couplings, described by a Hubbard model [26, 27],

$$H = H_\mu + H_t + H_U + H_J. \tag{1}$$

Here, $H_\mu = \sum_{i,\sigma} -(\mu_i + \varepsilon_i(\tau))n_{i,\sigma}$, where $\mu$ is the electrochemical potential of the $i$-th dot and $\varepsilon_i(\tau)$ is the experimentally controlled detuning energy of the $i$-th dot with time $\tau$. $n_{i,\sigma} = c^\dagger_{i\sigma}c_{i\sigma}$ is the electron number operator with spin $\sigma$. $H_t = -\sum_{<i,j>,\sigma} t\ c^\dagger_{i\sigma}c_{j\sigma}$ describe nearest neighbor interdot hopping. $H_U = \sum_i U_i n_{i,\uparrow}n_{i,\downarrow} + \sum_{<i,j>} U_{ij}n_{i,\uparrow}n_{j,\downarrow}$ describe the intradot Coulomb energy $U_i$ and interdot direct Coulomb energy $U_{ij}$. $H_J = -\frac{1}{2}\sum_{<i,j>} J_e c^\dagger_{i\downarrow}c^\dagger_{j\uparrow}c_{j\downarrow}c_{i\uparrow} + \sum_{i,\sigma} J_e n_{i,\sigma}n_{i,\sigma}$ is the spin exchange energy term. Both $J_e$ and $t$ are positive, real number-valued parameters. Eq. 1 assumes each quantum dot is either empty, singly or doubly occupied with both electrons in the ground orbital forming a spin singlet. This is justified because the excited orbital is well separated [28]. Furthermore, the effect of higher orbitals causes only a small renormalization of the Hubbard parameters [29].

For the ST qubit, an interdot magnetic field differ-

ence $\Delta B$ arises from nuclear spins [20] or micromagnets [18, 30], which together with the exchange $J_e$, offers control over two independent rotation axes on the qubit Bloch sphere. While there is no direct control over $\Delta B$, electrical control over detuning allows the qubit to be pulsed quickly into regimes where either exchange or magnetic coupling energies dominate. In this work, we consider the regime where the exchange energy dominates. The value of exchange we adopt is several orders of magnitude larger than typical experimental values of the magnetic energy term $g\mu_B\Delta B$ in Si: $\sim 3$ neV in natural Si [31] or $\sim 60$ neV with micromagnets [18]. Here, $g$ is the $g$-factor of the host semiconductor; $\mu_B$ is the Bohr magneton. In addition, the typical in-plane magnetic field affects the Zeeman energy of spin states outside the $S_z = 0$ basis, thus we exclude magnetic terms in Eq. 1.

In our numerical simulations, we use typical quantum dot parameters in agreement with experiments in Si quantum dots [32]. We assume identical dots with identical, constant nearest-neighbour tunnel and exchange couplings, $t = 0.12$ meV, $J_e = 0.1$ meV, from Ref. 27. We take identical intradot and nearest neighbor interdot Coulomb energies $U_i = U = 6.1$ meV [27] and $U_{ij} = K$.

*Schemes for State Transfer.–* The purpose of our proposed schemes is to coherently transfer an arbitrary superposition of the $S$ and $T_0$ states of the ST qubit from one end of a chain of otherwise empty quantum dots to the other end. Because the Hamitonian is spin conserving, it is block diagonal in spin space. However, even though the singlet and triplet states are uncoupled, without knowing the initial admixture of singlet and triplet states, the problem of state transfer is non-trivial due to the non-identical interdot coupling of the different spin and charge states, errors from phase accumulation, and leakage into states of undesired charge occupation.

We start with a general initial state in the first two quantum dots, $|\psi_0\rangle = \cos\theta\,|S\rangle_{1,2} + e^{i\phi}\sin\theta\,|T_0\rangle_{1,2}$, where $|S/T_0\rangle_{i,j} = (|\uparrow_i\downarrow_j\rangle \mp |\downarrow_i\uparrow_j\rangle)/\sqrt{2}$. Indices $i(j)$ refer to quantum dots $i(j)$, $\theta$ determines the admixture of the singlet and triplet states, and $\phi$ is the initial phase difference. The aim of the coherent state transfer is then to obtain the target state $|\psi_t\rangle = \cos\theta\,|S\rangle_{N-1,N} + e^{i\phi}\sin\theta\,|T_0\rangle_{N-1,N}$, for a chain of $N$ dots (Fig. 1(a)).

To reduce the problem, we start with the simplest, non-trivial case of $N = 3$, then extend it to arbitrary $N$ by considering the problem of state transfer across three consecutive dots at any one time, as sketched in Fig. 1(a). The fidelity of state transfer [33] is $\mathcal{F} = |\langle\psi_t\,|\,\psi_f(\tau_f)\rangle|^2$, where $|\psi_f(\tau_f)\rangle$ is the final state at time $\tau_f$.

With $N = 3$ and one ground orbital in each dot, the basis states comprise 3 different charge states within the unpolarized triplet spin space $\{|T_0\rangle_{1,2}, |T_0\rangle_{1,3}, |T_0\rangle_{2,3}\}$ and 6 singly- and doubly-occupied charge states within the singlet spin space $\{|S\rangle_{1,2}, |S\rangle_{1,3}, |S\rangle_{2,3}, |S\rangle_{1,1}, |S\rangle_{2,2}, |S\rangle_{3,3}, \}$. In all our numerical simulations, we use the Hamiltonian in Eq. 1 in this 9-dimensional basis [34].

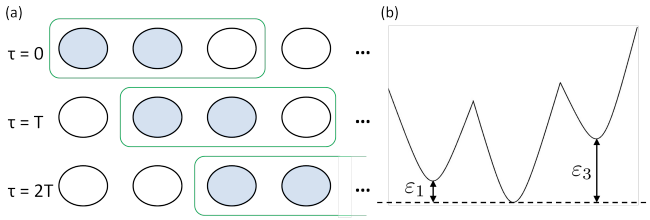


FIG. 1. Schematic of state transfer. (a) Circles indicate quantum dots. Shaded circles indicate that the dots are filled with an electron. We consider three dots at each time during the state transfer, as indicated by the green boxes. State transfer times $\tau$ scale linearly: $\tau = T$ and $\tau = 2T$ for 3 and 4 dots. (b) Schematic of the confinement potentials of three dots and the detuning energies of the first and third dot, $\varepsilon_1$ and $\varepsilon_3$.

*Pulse-Gated Scheme.–* In the implementation of the pulse-gated state transfer scheme, dc square pulses are applied to control the detuning energies $\varepsilon_i$. The pulse sequence moves the dots between the following regimes: (I) where the right dot is far detuned from the other dots ($\varepsilon_3 \gg \varepsilon_1, \varepsilon_2$); (II) where the left and right dots are on resonance, but detuned from the middle dot ($\varepsilon_1 = \varepsilon_3 = \varepsilon > \varepsilon_2$); and then to regime (III) where the left dot is far detuned from the other dots ($\varepsilon_1 \gg \varepsilon_3, \varepsilon_2$). In the far-detuned regime (I), the two lowest lying states are $|S\rangle_{1,2}$ and $|T_0\rangle_{1,2}$, as sketch in Fig. 2(a).

In regime (II), $|S/T_0\rangle_{1,2}$ and $|S/T_0\rangle_{2,3}$ are brought into resonance with each other via control over the detuning energies of dots 1 and 3. The initial and target singlet and triplet states are coupled via intermediate states $|S\rangle_{1,3}$ and $|S\rangle_{2,2}$, and $|T_0\rangle_{1,3}$. These couplings are shown in black arrows in Fig. 2(b). The singlet states also couple to leakage states of undesired charge occupation $|S\rangle_{1,1}$ and $|S\rangle_{3,3}$, shown in grey arrows. The Schrieffer-Wolff transformation [34–37] gives some insight into the effective couplings between the initial and target singlet and triplet states. They are given respectively by $J_S = -t^2\left(\frac{-4}{U-K+\varepsilon} + \frac{2}{K+\varepsilon}\right)$, and $J_T = -t^2\left(\frac{2}{K+\varepsilon}\right)$. This implies that for a pure singlet or triplet initial state, by waiting in regime (II) for a time of $\tau = \hbar\pi/J_{S/T}$, the target state may be reached with the highest fidelity. However, if the initial state is an unknown superposition of singlet and triplet, for maximum fidelity with both spin states simultaneously transferred, the gating times must be equal, or $J_S = J_T = J$. This condition is satisfied by requiring the ratio of the intra- to inter-dot Coulomb repulsion to be $U/K = 2$. We emphasize that the SW transformation is used to gain insight only and we do not use the effective SW Hamiltonian in our simulations.

In our numerical study for this scheme, we use parameter value of $K = 3.05$ meV $= U/2$ [27], detuning energies

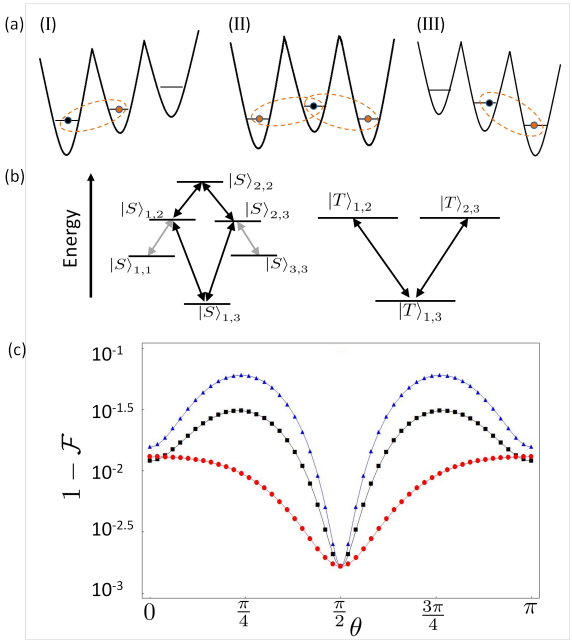


FIG. 2. Pulse-gated scheme for ST qubit state transfer for three dots. (a) Schematic of the detunings in regimes (I, II, III) according to Eq. 2. Electrons are represented by filled circles; black horizontal lines represents the ground orbitals. Detuning pulses move the dots in the following sequence: the system begins in regime (I) where the right dot is far detuned from the other dots; it is pulsed to regime (II) where the left and right dots are on resonance, and where state transfer takes place; then it goes into regime (III) where the left dot is far detuned and an additional wait time corrects phase errors. In (I) and (III), the two lowest lying states are the $S$ and $T_0$ states of the two leftmost and rightmost dots respectively as represented by dashed ellipses. In regime (II), the left and right dots are on resonance, allowing state transfer between the $|S,T_0\rangle_{1,2}$ and $|S,T_0\rangle_{2,3}$ states (dashed ellipses). (b) Tunnel couplings are shown as arrows, sketched against a vertical energy axis (not to scale). Tunnel couplings shown in black arrows link the initial and target states via intermediate states. Tunnel couplings in grey link to leakage states. (c) Plot of infidelity $1-\mathcal{F}$ with mixing angle $\theta$ for $\delta=0$ (red circles), $\delta=0.01(2K)$ (black squares) and $\delta=-0.01(2K)$ (blue triangles), where $U=2K+\delta$, $K=3.05$ meV and $t=0.12$ meV. The fidelity, $\mathcal{F}$ has a value of $98.7\%<\mathcal{F}<99.8\%$ for all $\theta$ with a transfer time of $T=0.58$ ns.

$\varepsilon_2=0$ and

$$\varepsilon_{3/1}=\begin{cases} -/+D_{\rm p} & ,\tau<-\hbar\pi/2J & :\text{(I)} \\ \varepsilon & ,-\hbar\pi/2J\le\tau\le\hbar\pi/2J & :\text{(II)} \\ +/-D_{\rm p} & ,\tau>\hbar\pi/2J & :\text{(III)} \end{cases} ,(2)$$

where $\varepsilon=5$ meV and $D_{\rm p}=10$ meV.

After the pulse sequence is completed, an additional wait time of $\tau_{\rm wait}$ is required to correct for the difference in the dynamical phase accumulation between singlet and triplet states during regime (II). This is due to the small difference in the singlet and triplet state energies. From a numerical search, we find that $\tau_{\rm wait}\approx 3\hbar/\varepsilon$ allows optimal fidelity across the range of mixing angles $\theta$.

Finally, we plot the infidelity $1-\mathcal{F}$, of the pulse-gated scheme for various mixing angles $\theta$ of the initial state, and $\phi=0$, in Fig. 2(c) (red circles). The transfer fidelity obtained is then given by $98.7\%<\mathcal{F}<99.8\%$ with a transfer time of $T=\hbar\pi/J+\tau_{\rm wait}\approx 0.58$ ns. Perfect state transfer is not achieved primarily due to the leakage into other, non-target charge states of the system Hilbert space. Similar fidelities and rates are obtained for other values of initial phase $\phi$ using the same parameters [34].

For the non-ideal situation where $U=2K+\delta$, with $\delta=\pm 0.01(2K)$, there is a reduction in fidelity across $\theta$ of a factor of approximately 10, except at $\theta=\pi/2$ which corresponds to a pure initial triplet (Fig. 2(c)).

*Adiabatic state transfer.–* In the second scheme, the initial state can be adiabatically evolved to the desired target state by tuning the detuning energies. Although adiabatic evolution is much slower in general, this scheme provides an alternative in the case that the desired Coulomb energies ratio $U/K$ is not met for pulse-gating. We consider the interdot Coulomb interaction strength of $K=2.3$ meV [27] while keeping experimentally realistic values for intra-dot Coulomb interaction strength and the other parameters the same in this scheme.

For adiabatic evolution, we propose a simple linear ramp of the detuning of the first and third dots $\varepsilon_{1,3}$, while keeping the detuning of the second dot $\varepsilon_2$ constant. This is shown in Fig. 3(a) and Table I. The system goes through regimes (I', II' and III'), similar (but not identical) to the pulse-gated scheme. The system starts in the singlet and triplet ground states in regime (I'), evolves adiabatically through regime (II') through avoided crossings, and ends in regime (III') with a wait time $\tau_{\rm wait}$ to correct phase errors.

The avoided crossings occur at $\varepsilon_3(\tau)-\varepsilon_1(\tau)=0$, as shown in Fig. 3(b,c). As shown in Fig. 3(b), the avoided crossings for singlets arises from the tunnel couplings between $|S\rangle_{1,2}$ and $|S\rangle_{2,3}$ with $|S\rangle_{2,2}$, while the avoided crossing for triplets (Fig. 3(c)) arises from the tunnel couplings between $|T_0\rangle_{1,2}$ and $|T_0\rangle_{2,3}$ with $|T_0\rangle_{1,3}$. Therefore, the energy gap for singlets and triplets are, respectively, $\varepsilon_{\rm gap,S}\sim\mathcal{O}(t)$, and $\varepsilon_{\rm gap,T}\sim\mathcal{O}(t^2/(\varepsilon+K))$, with $\varepsilon_{\rm gap,T}<\varepsilon_{\rm gap,S}$. The triplet energy gap $\varepsilon_{\rm gap,T}$ therefore sets an upper bound on adiabatic state transfer time, $R$.

A numerical simulation of the adiabatic state trans-

| | (I') $\tau<0$ | (II') $0\le\tau\le R$ | (III') $\tau>R$ |
|---|---|---|---|
| $\varepsilon_1$ (meV) | $-1$ | $-\frac{(D_{\rm ad}-1)\tau}{R\hbar}-1$ | $-D_{\rm ad}$ |
| $\varepsilon_2$ (meV) | $-1$ | $-1$ | $-1$ |
| $\varepsilon_3$ (meV) | $-D_{\rm ad}$ | $\frac{(D_{\rm ad}-1)\tau}{R\hbar}-D_{\rm ad}$ | $-1$ |

TABLE I. $D_{\rm ad}=8$ meV is the amplitude of the detunings and $R$ defines the time interval and therefore the rate of adiabatic evolution. During this time, the detuning energies of the first and third dots change linearly with time.

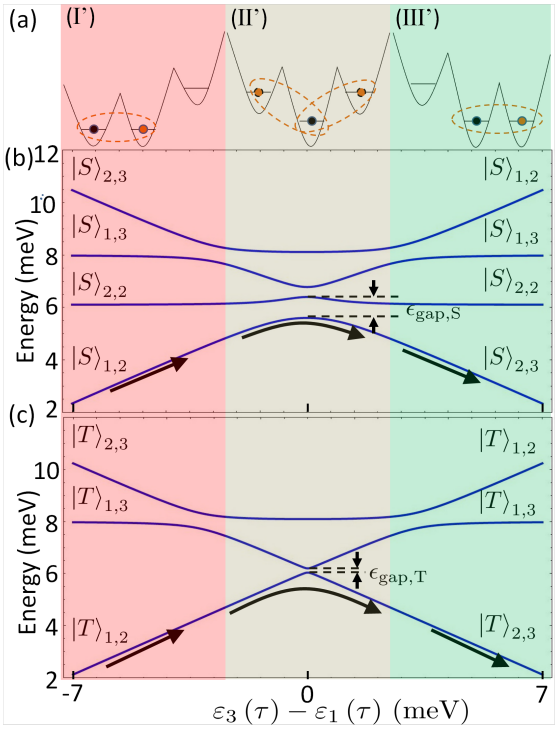


FIG. 3. Adiabatic state transfer scheme. (a) Schematic of the detuning of the quantum dots according to Table I. The dots start in regime (I') and the application of a linear ramp to detunings $\varepsilon_{1,3}$ move the left and right dots through the resonance condition $\varepsilon_1 = \varepsilon_3$ as shown in the middle panel. The dots end up in regime (III'). (b) The energies of the singlet and triplet states as a function of $\varepsilon_3(\tau) - \varepsilon_1(\tau)$. At far-detuned regimes of (I', III'), charge occupation of the dots are good eigenstates, and the system starts in an arbitrary superposition of the ground $|S, T_0\rangle_{1,2}$ states. As the detuning is sweep along the direction of the black arrows through regime (II') to (III'), the system evolves adiabatically to $|S, T_0\rangle_{2,3}$, with singlet and triplet states picking up different phase contributions. Similar to the pulse-gated scheme, an additional wait time at the end of regime (III') corrects the phase error.

fer for different values for $\theta$ and $\phi$ was performed for $R = 65.8$ ns. In the absence of noise, an infinitely long state transfer would yield arbitrarily high fidelities. Here, the choice of $R$ to be of the same order of magnitude of dephasing times in silicon dots [38] is intentional as we expect realistic state transfer times to be bounded by dephasing time. The wait time after the detuning pulses (Table I), $\tau_{\mathrm{wait}} \approx 12\hbar/\varepsilon$ was found numerically to correct for the phase difference accumulated by the singlet and triplet states. The plot of the infidelity $1 - \mathcal{F}$ across $\theta$, for $\phi = 0$, is shown in Fig. 4 for the adiabatic scheme (blue squares), and overlap the infidelity for the pulse-gated scheme (red circles). The latter is identical to the same plot in Fig. 2(c) for $\delta = 0$. As may be expected, the adiabatic scheme gives slightly better fidelity of at least 99.3%, but at a cost of longer transfer times $T = R + \tau_{\mathrm{wait}} \approx 65.8$ ns. Without changing the $\tau_{\mathrm{wait}}$,

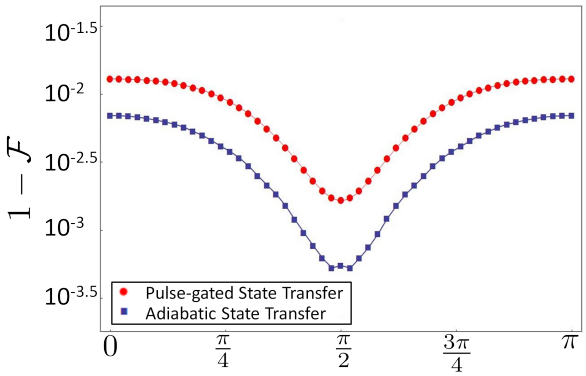


FIG. 4. Plot of infidelity $1-\mathcal{F}$ against mixing angle $\theta$. Results of numerical simulations of the adiabatic state transfer scheme (blue squares) is plotted together with that of the pulse-gated scheme (red circles), the latter being identical to the same plot in Fig. 2(c). Both schemes give fidelities in excess of 98.7% across $\theta$, with subnanosecond transfer times $T = 0.58$ ns for the pulse-gated scheme, and 99.3% across $\theta$ for $T = 65.8$ ns for the adiabatic scheme.

identical fidelities for all values of $\theta$ can be obtained for arbitrary values of $\phi$ [34].

*Generalization to N dots.*– By having sufficiently large detunings for three consecutive dots from the rest of the chain, triple dots can be isolated energetically. In this way, state transfer can be generalized to $N > 3$. For a state transfer time of $T$ with three dots, the required time for a chain of $N > 3$ dots is $(N - 2)$ T [34].

*Summary.*– In summary, we presented two experimentally feasible schemes for ST qubit state transfer in a linear chain of quantum dots in order to address the important issue of the transfer of quantum information in the scaling up of ST qubits. For $N = 3$, the pulse-gated scheme gives a fidelity of at least 98.7% across $\theta$ within a short transfer time of 0.58 ns, by requiring $U/K = 2$. Adiabatic state transfer allows for slightly higher fidelity of at least 99.3% at a longer time, but without the condition on the Coulomb energies ratio. We showed that the state transfer schemes can be generalized to longer chains by isolating three dots at each time.

*Acknowledgement.*– We thank David P. DiVincenzo for helpful discussions. This work was supported by the National Research Foundation and Ministry of Education, Singapore.

[1] F. H. L. Koppens, C. Buizert, K. J. Tielrooij, I. T. Vink, K. C. Nowack, T. Meunier, L. P. Kouwenhoven, and L. M. K. Vandersypen, Nature **442**, 766 (2006).
[2] H. Bluhm, S. Foletti, I. Neder, M. Rudner, D. Mahalu, V. Umansky, and A. Yacoby, Nature Physics **7**, 109 (2011).
[3] D. Loss and D. P. DiVincenzo, Phys. Rev. A **47**, 120 (1998).

[4] J. Levy, Phys. Rev. Lett. **89**, 147902 (2002).
[5] J. R. Petta, H. Lu, and A. C. Gossard, Science **327**, 669 (2010).
[6] D. P. DiVincenzo, D. Bacon, J. Kempe, G. Burkard, and K. B. Whaley, Nature **408**, 339 (2000).
[7] E. A. Laird, J. M. Taylor, D. P. DiVincenzo, C. M. Marcus, M. P. Hanson, and A. C. Gossard, Phys. Rev. B **82**, 075403 (2010).
[8] K. M. Svore, B. M. Terhal, and D. P. DiVincenzo, Phys. Rev. A **72**, 022317 (2005).
[9] Q. Li, L. Cywinski, D. Culcer, X. Hu, and S. Das Sarma, Phys. Rev. B **81**, 085313 (2010).
[10] J. M. Taylor, H.-A. Engel, W. Dür, A. Yacoby, C. M. Marcus, P. Zoller, and M. D. Lukin, Nature Physics **1**, 177 (2005).
[11] M. Christandl, N. Datta, A. Ekert, and A. J. Landahl, Phys. Rev. Lett. **92**, 187902 (2004).
[12] M. Friesen, A. Biswas, X. Hu, and D. Lidar, Phys. Rev. Lett. **98**, 230503 (2007).
[13] A. D. Greentree, J. H. Cole, A. R. Hamilton, and L. C. L. Hollenberg, Phys. Rev. B **70**, 235317 (2004).
[14] E. Ferraro, M. D. Michielis, M. Fanciulli, and E. Prati, Phys. Rev. B **91**, 075435 (2015).
[15] A. Imamoglu, D. D. Awschalom, G. Burkard, D. P. DiVincenzo, D. Loss, M. Sherwin, and A. Small, Phys. Rev. Lett. **83**, 4204 (1999).
[16] X. Hu, Y.-X. Li, and F. Nori, Phys. Rev. B **86**, 035314 (2012).
[17] K. D. Petersson, L. W. McFaul, M. D. Schroer, M. Jung, J. M. Taylor, A. A. Houck, and J. R. Petta, Nature **490**, 380 (2012).
[18] X. Wu, D. R. Ward, J. R. Prance, D. Kim, J. Gamble, R. T. Mohr, Z. Shi, D. E. Savage, M. G. Lagally, M. Friesen, S. N. Coppersmith, and M. A. Eriksson, Proc. Nat. Acad. Sci. **111**, 11938 (2014).
[19] M. D. Shulman, O. E. Dial, S. P. Harvey, H. Bluhm, V. Umansky, and A. Yacoby, Science **336**, 202 (2012).
[20] B. M. Maune, M. G. Borselli, B. Huang, T. D. Ladd, P. W. Deelman, K. S. Holabird, A. A. Kiselev, I. Alvarado-Rodriguez, R. S. Ross, A. E. Schmitz, M. Sokolich, C. A. Watson, M. F. Gyure, and A. T. Hunter, Nature **481**, 344 (2012).
[21] D. J. Reilly, J. M. Taylor, J. R. Petta, C. M. Marcus, M. P. Hanson, and A. C. Gossard, Science **321**, 817 (2008).
[22] S. Foletti, H. Bluhm, D. Mahalu, V. Umansky, and A. Yacoby, Nature Physics **5**, 903 (2009).
[23] F. A. Zwanenburg, A. S. Dzurak, A. Morello, M. Y. Simmons, L. C. L. Hollenberg, G. Klimeck, S. Rogge, S. N. Coppersmith, and M. A. Eriksson, Rev. Mod. Phys. **85**, 961 (2013).
[24] C. Tahan, M. Friesen, and R. Joynt, Phys. Rev. B **66**, 035314 (2002).
[25] S. Bose, Contemp. Phys. **48**, 13 (2007).
[26] S. Yang, X. Wang, and S. Das Sarma, Phys. Rev. B **83**, 161301 (2011).
[27] S. Das Sarma, X. Wang, and S. Yang, Phys. Rev. B **83**, 235314 (2011).
[28] X. Hu and S. Das Sarma, Phys. Rev. A **61**, 062301 (2000).
[29] X. Wang, S. Yang, and S. Das Sarma, Phys. Rev. B **84**, 115301 (2011).
[30] M. Pioro-Ladriere, T. Obata, Y. Tokura, Y.-S. Shin, T. Kubo, K. Yoshida, T. Taniyama, and S. Tarucha, Nature Physics **4**, 776 (2008).
[31] L. V. C. Assali, H. M. Petrilli, R. B. Capaz, B. Koiller, X. Hu, and S. Das Sarma, Phys. Rev. B **83**, 165301 (2011).
[32] C. B. Simmons, M. Thalakulam, B. M. Rosemeyer, B. J. van Bael, E. K. Sackmann, D. E. Savage, M. G. Lagally, R. Joynt, M. Friesen, S. N. Coppersmith, and M. A. Eriksson, Nano Lett. **9**, 3234 (2009).
[33] R. Josza, J. Mod. Optics **41**, 2315 (1994).
[34] See Supplemental Information for more details.
[35] J. R. Schrieffer and P. A. Wolf, Physical Review **149**, 491 (1966).
[36] C. Gros, R. Joynt, and T. M. Rice, Phys. Rev. B **36**, 381 (1987).
[37] A. H. MacDonald, S. M. Girvin, and D. Yoshioka, Phys. Rev. B **37**, 9753 (1988).
[38] Z. Shi, C. B. Simmons, D. R. Ward, J. R. Prance, X. Wu, T. S. Koh, J. K. Gamble, D. E. Savage, M. G. Lagally, M. Friesen, S. N. Coppersmith, and M. A. Eriksson, Nature Communications **5**, 3020 (2013).

arXiv:1602.08596v1 [quant-ph] 27 Feb 2016

# *Supplemental Material:* Coherent transfer of singlet-triplet qubit states in a scalable architecture of linear quantum dots

Chang Jian Kwong
*Centre for Quantum Technologies, National University of Singapore, 3 Science Drive 2, Singapore 117543, Singapore*

Teck Seng Koh
*Ministry of Education, 1 North Buona Vista Drive, Singapore 138675, Singapore*

Leong Chuan Kwek
*Centre for Quantum Technologies, National University of Singapore, 3 Science Drive 2, Singapore 117543, Singapore*
*Institute of Advanced Studies, Nanyang Technological University,*
*60 Nanyang View, Singapore 639673, Singapore and*
*National Institute of Education, Nanyang Technological University, 1 Nanyang Walk, Singapore 637616, Singapore*

## SCHRIEFFER WOLFF TRANSFORMATION

The Hamiltonian describing a multi-dots linear chain system is given by

$$\hat{H} = \hat{H}_\mu + \hat{H}_t + \hat{H}_U + \hat{H}_J,$$

where $\hat{H}_\mu$ is the chemical potential, $\hat{H}_t$ is the hopping term, $\hat{H}_U$ is the intradot and interdot Coulomb potential and $\hat{H}_J$ is the spin exchange interaction term. Each components of the Hamiltonian are given by

$$\begin{aligned}
\hat{H}_\mu &= \sum_{i,\sigma} -(\mu_i + \varepsilon_i(\tau)) n_{i,\sigma} \\
\hat{H}_t &= \sum_{<i,j>,\sigma} \left( -t c^\dagger_{i\sigma} c_{j\sigma} + \text{H.c.} \right) \\
\hat{H}_U &= \sum_i U_i n_{i,\uparrow} n_{i,\downarrow} + \frac{1}{2} \sum_{<i,j>} U_{ij} (n_{i,\uparrow} n_{j,\downarrow} + n_{j,\downarrow} n_{i,\uparrow}) \\
\hat{H}_J &= -\frac{1}{2} \sum_{<i,j>} J_e c^\dagger_{i\downarrow} c^\dagger_{j\uparrow} c_{j\downarrow} c_{i\uparrow}.
\end{aligned}$$

The Hamiltonian can be categorised into Coulomb interaction consisting of the inter-dot and intra-dot Coulomb interaction with the tunneling, exchange interaction and the detunings treated as perturbation. For the singlet states, the basis states are

$$\begin{aligned}
|S\rangle_{3,3} &= |\uparrow_3 \downarrow_3\rangle \\
|S\rangle_{2,3} &= \frac{1}{\sqrt{2}} \left( |\uparrow_2 \downarrow_3\rangle - |\downarrow_2 \uparrow_3\rangle \right) \\
|S\rangle_{1,3} &= \frac{1}{\sqrt{2}} \left( |\uparrow_1 \downarrow_3\rangle - |\downarrow_1 \uparrow_3\rangle \right) \\
|S\rangle_{2,2} &= |\uparrow_2 \downarrow_2\rangle \\
|S\rangle_{1,2} &= \frac{1}{\sqrt{2}} \left( |\uparrow_1 \downarrow_2\rangle - |\downarrow_1 \uparrow_2\rangle \right) \\
|S\rangle_{1,1} &= |\uparrow_1 \downarrow_1\rangle ,
\end{aligned}$$

while the basis states for triplet staes are

$$\begin{aligned}
|T_0\rangle_{1,2} &= \frac{1}{\sqrt{2}} \left( |\uparrow_1 \downarrow_2\rangle + |\downarrow_1 \uparrow_2\rangle \right) \\
|T_0\rangle_{1,3} &= \frac{1}{\sqrt{2}} \left( |\uparrow_1 \downarrow_3\rangle + |\downarrow_1 \uparrow_3\rangle \right) \\
|T_0\rangle_{2,3} &= \frac{1}{\sqrt{2}} \left( |\uparrow_2 \downarrow_3\rangle + |\downarrow_2 \uparrow_3\rangle \right) .
\end{aligned}$$

Accordingly, the Hamiltonian can then be written in matrix given by

$$\hat{H}_S = \begin{pmatrix}
U - 2(\varepsilon_3 + \mu) & -\sqrt{2}t & 0 & 0 & 0 & 0 \\
-\sqrt{2}t & J_e + U_{12} - \varepsilon_2 - \varepsilon_3 - 2\mu & -t & -\sqrt{2}t & 0 & 0 \\
0 & -t & -(\varepsilon_1 + \varepsilon_3 + 2\mu) & 0 & -t & 0 \\
0 & -\sqrt{2}t & 0 & U - 2(\varepsilon_2 + \mu) & -\sqrt{2}t & 0 \\
0 & 0 & -t & -\sqrt{2}t & J_e + U_{12} - \varepsilon_1 - \varepsilon_2 - 2\mu & -\sqrt{2}t \\
0 & 0 & 0 & 0 & -\sqrt{2}t & U - 2(\varepsilon_1 + \mu)
\end{pmatrix}$$

$$\hat{H}_T = \begin{pmatrix}
-J_e + U_{12} - \varepsilon_1 - \varepsilon_2 - 2\mu & -t & 0 \\
-t & -(\varepsilon_1 + \varepsilon_3 + 2\mu) & -t \\
0 & -t & -J_e + U_{12} - \varepsilon_2 - \varepsilon_3 - 2\mu
\end{pmatrix},$$

where $\hat{H}_S$ is the Hamiltonian for singlet states and $\hat{H}_T$ is the Hamiltonian for triplet states. Together, they form

a block diagonal Hamiltonian $\hat{H}$ since the singlet and triplet states do not mixed due to the absence of spin-orbit coupling and magnetic field.

For Schrieffer-Wolff transformation [1, 2], we have

$$\begin{aligned}\hat{H}_{\text{eff}} &= e^{iS}\hat{H}e^{-iS} \\ &= \hat{H} + \left[iS, \hat{H}\right] \\ &= \hat{H}_U + \hat{H}_T + \left[iS, \hat{H}_U\right] + \left[iS, \hat{H}_t + \hat{H}_J\right] + ...,\end{aligned}$$

where $\hat{H}_T = \hat{H}_t + \hat{H}_J$ and we require $\hat{H}_T + \left[iS, \hat{H}_U\right] = 0$. This can be done by choosing the operator, $iS = \sum_{n,m} \langle\psi_n| \hat{H}_T |\psi_m\rangle / \left(\langle\psi_n| U |\psi_n\rangle - \langle\psi_m| U |\psi_m\rangle\right) |\psi_n\rangle \langle\psi_m|$ with $|\psi_n\rangle$ are the eigenstates of the diagonal Hamiltonian of the Coulomb interaction, $\hat{H}_U$ [2]. As a result, the effective Hamiltonian obtained is block diagonalised. With the given choice of the operator $S$, we have

$$\begin{aligned}\langle\psi_k| \left[iS, \hat{H}_t + \hat{H}_J\right] |\psi_l\rangle = &\sum_m \frac{\langle\psi_k| \hat{H}_T |\psi_m\rangle \langle\psi_m| \hat{H}_T |\psi_l\rangle}{U_k - U_m} \\ &- \sum_m \frac{\langle\psi_k| \hat{H}_T |\psi_m\rangle \langle\psi_m| \hat{H}_T |\psi_l\rangle}{U_m - U_l}.\end{aligned}$$

The effective Hamiltonian is then given by $\hat{H}_{\text{eff}} = \hat{H}_U + \left[iS, \hat{H}_T\right]$. From $\hat{H}_{\text{eff}}$, the effective coupling between the initial state and the final state, i.e. second order transition, for both the singlet and triplet states can be obtained.

$$J_S = -t^2\left(\frac{-4}{U - K + \varepsilon} + \frac{2}{K + \varepsilon}\right) \quad (1)$$

$$J_T = -t^2\left(\frac{2}{K + \varepsilon}\right) \quad (2)$$

where $J_S$ is the effective coupling between $|S\rangle_{1,2}$ and $|S\rangle_{2,3}$ while $J_T$ is the effective coupling between $|T_0\rangle_{1,2}$ and $|T_0\rangle_{2,3}$.

## STATE EVOLUTION WITHOUT DETUNING CONTROL

In the absence of control over detunings, state transfer can be implemented by initialising the singlet-triplet qubit at one end and letting the system evolve with time. Then, the state evolution is stopped and quantum gate operations or read out measurements can be performed immediately. The initial state is initialised in dots 1 and 2 with the state

$$|\psi_0\rangle = \cos\theta\,|S\rangle_{1,2} + \sin\theta e^{i\phi}\,|T_0\rangle_{1,2} \quad (3)$$

where $|S\rangle_{i,j} = \frac{1}{\sqrt{2}}(|\uparrow\downarrow\rangle_{i,j} - |\downarrow\uparrow\rangle_{i,j})$ and $|T_0\rangle_{i,j} = \frac{1}{\sqrt{2}}(|\uparrow\downarrow\rangle_{i,j} + |\downarrow\uparrow\rangle_{i,j})$ with the indices $i(j)$ referring to the quantum dots $i(j)$ and $\theta$ determines the component of the singlet and triplet states of the initial state. Here, we assume $\phi = 0$ without loss of generality. The state transfer for initial states with relative phase between the singlet and triplet states, where $\phi = \pi/4$ and $\phi = \pi/6$, are demonstrated in Sec. for the pulse-gated scheme. The state is then allowed to evolve with time and stopped upon achieving coherent state transfer with a fidelity that is higher than 0.7 for all initial states. The definition for fidelity and average fidelity are given by

$$\mathcal{F} = |\langle\psi_t\,|\,\psi_f\rangle|^2, \quad \mathcal{F}_{\text{ave}} = \frac{1}{2}\int_0^\pi \mathrm{d}\theta\mathcal{F}(\theta,\tau)\sin\theta,$$

where $\tau$ is the instantaneous time, $\theta$ determines the initial state and $|\psi_f\rangle$ is the final state of the singlet-triplet qubit.

Hence, the average fidelity which is averaged over all initial states can be plotted against evolution time. Assuming that the quantum dots are on resonance, Fig.

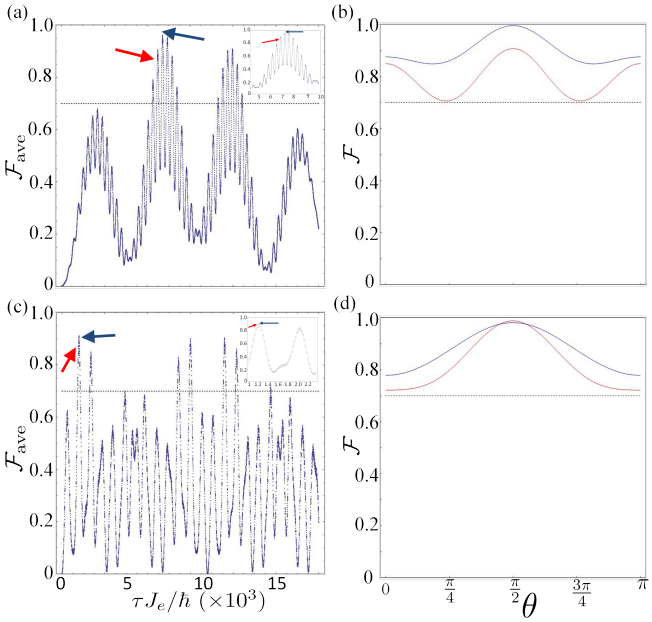


FIG. 1. (Colour Online) (a) Average fidelity for $t = 0.12$ meV. The blue arrow indicates the highest peak within an interval of 1.2 ns at 0.47 ns while red arrow gives the earliest coherent state transfer achievable via free evolution at 0.45 ns. (b) The fidelity for both times indicating that the state transfer exceed the classical limit of efficiency of quantum transfer. The tunnel coupling is $t = 0.12$ meV. (c) Average fidelity for $t = 0.3$ meV. The blue arrow indicates the highest average fidelity at 81 ps and earliest coherent state transfer achievable at 77 ps. (d) The fidelity calculated from the system with tunneling, $t = 0.3$ meV for comparison.

1 shows the average fidelity plotted from 0 to 1.2 ns for (a) $t = 0.12$ meV and (c) $t = 0.30$ meV. The highest peak in Fig. 1 (a) is at 0.47 ns (blue arrow) with an average fidelity of 0.96 while the shortest evolution time is 0.45 ns (red arrow). Corresponding to these two times, the fidelity for all $\theta$ is plotted in Fig. 1 (b), demonstrating that the fidelity is above the threshold of 0.7 for all initial states. Hence, with free evolution, we can already obtain

a state transfer that is better than the classical limit for the efficiency.

In comparisons, the envelope in Fig. 1 (a) is absent from Fig. 1 (c) due ot its faster state evolution. The higher tunnel coupling allows a higher probability for the electrons to tunnel between adjacent quantum dots leading to a faster state evolution. This in turn leads to shorter time required for coherent state transfer as seen in highest peak at 81 ps (blue arrow) in Fig. 1 (c) with an average fidelity of 0.91 and shortest time evolution of 77 ps (red arrow). In addition, the faster state evolution also leads to lower fidelity. Fig. 1 (d) shows the fidelity corresponding to the highest average fidelity as well as the earliest instance of coherent state transfer. From the numerical simulation of the $N = 3$ dots linear chain, we have found the required evolution time to achieve coherent state transfer. However, as we have seen from the results, the fidelity obtained is less than desirable. Hence, we require the adiabatic and pulse gate state transfer scheme in order to have high fidelity state transfer.

## PULSE-GATED SCHEME WITH DIFFERENT PARAMETERS

A different set parameters for the Coulomb interactions, i.e. $U = 4.6$ meV and $K = 2.3$ meV, while the resonant detunings of dots 1 and 3, $\epsilon = 5$ meV is used. Due to the change in the parameters, the transfer time is different with a slightly longer time of 0.74 ns. In addition, the change in the parameters causes a change in the energy level thereby together with the difference in transfer time, caused a different dynamical phase accumulated during the state transfer. As a result, the required wait time is found to be given by $\tau_{\text{wait}} \approx 12\hbar/\varepsilon$.

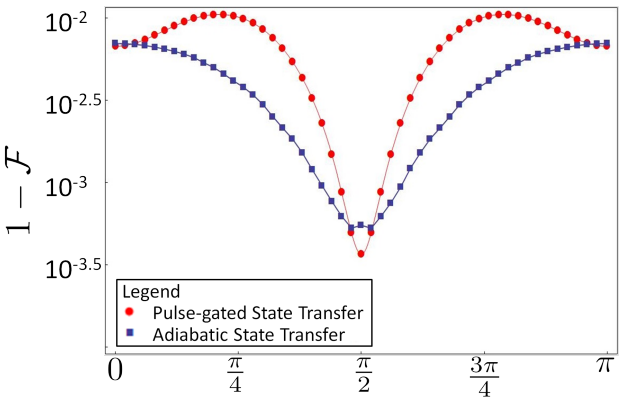


FIG. 2. (Colour Online) Plot of infidelity, $1 - \mathcal{F}$ against mixing angle $\theta$. The results for pulse-gated scheme (red circles) are compared with the simulation results of the adiabatic scheme (blue squares). We observed that similar to the results in the main text, the pulse-gated scheme generally has a lower state transfer fidelity. However, the state transfer time is shorter with approximately 0.74 ns transfer time.

## INITIAL STATES WITH RELATIVE PHASE

In this section, we investigate the state transfer for initial states with $\phi = \pi/6$ and $\phi = \pi/4$. The wait time, $\tau_{\text{wait}}$ is found numerically to be approximately $3\hbar/\varepsilon$ for all values of $\phi$. Fig. 3 shows the plot of infidelities for both cases as well as the case of $\phi = 0$. There is no visible difference between the plot of infidelities obtained for arbitrary values of $\phi$. This is due to the identical fidelities obtained with the same system parameters and wait time.

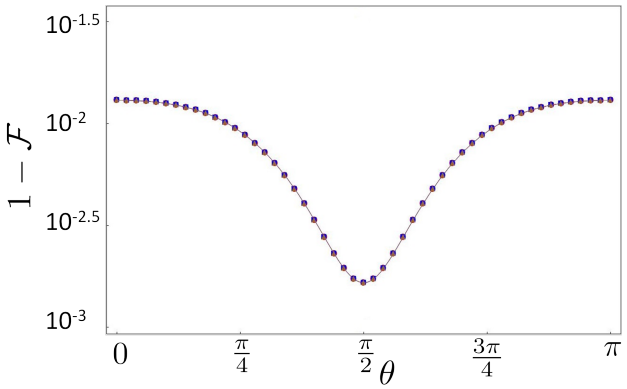


FIG. 3. (Colour Online) Plot of infidelity, $1 - \mathcal{F}$ for the initial states with $\phi = 0$ (brown triangle), $\phi = \pi/6$ (blue squares) and $\phi = \pi/4$ (red circles). The infidelity obtained suggests that state transfer for any arbitrary initial state of $|S\rangle_{1,2}$ and $|T_0\rangle_{1,2}$ with relative phase, $\phi$ can be achieved with high fidelity via the pulse-gated state transfer. With the same wait time, $\tau_{\text{wait}}$ and system parameters, the fidelities obtained are identical for any arbitrary values of $\phi$.

Similarly, the simulation for adiabatic scheme for the state transfer for $\phi = \pi/6$ and $\phi = \pi/4$ are carried out. The plot of infidelities for all three cases including $\phi = 0$ are shown in Fig. 4. Here, we show only the results for $\phi = \pi/6$ and $\phi = \pi/4$ as an example to illustrate that both the adiabatic and pulse-gated state transfer schemes can be implemented irrespective of the initial relative phase of the singlet-triplet qubit. In addition, with the same $\tau_{\text{wait}}$, the fidelities obtained are identical to each other for arbitrary values of $\phi$.

## LEADING ORDER ERROR IN PULSE GATE SCHEME

In the pulse gate scheme, we impose a condition where $U = 2U_{12}$. In order to find out the leading error term, consider a perturbation on the intradot Coulomb interaction, where $U = 2U_{12} + \delta U$. As a result, the singlet

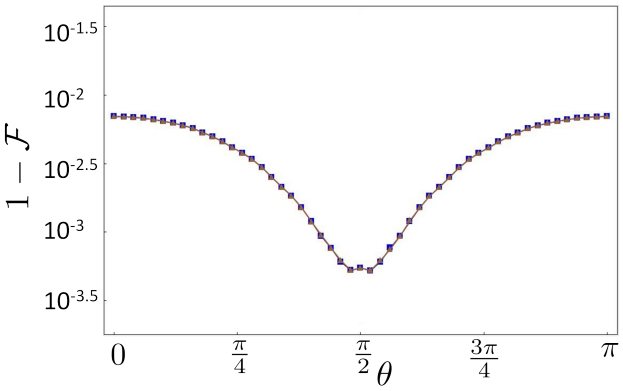


FIG. 4. (Colour Online) Plot of infidelity, $1-\mathcal{F}$ for the initial states with $\phi = 0$ (brown triangle), $\phi = \pi/6$ (blue squares) and $\phi = \pi/4$ (red circles). The infidelity obtained suggests that state transfer for any arbitrary initial state of $|S\rangle_{1,2}$ and $|T_0\rangle_{1,2}$ with relative phase, $\phi$ can be achieved with high fidelity via the adiabatic state transfer. With the same wait time, $\tau_{\text{wait}}$ and system parameters, the fidelities obtained are identical for any arbitrary values of $\phi$.

states effective coupling are then given by

$$\begin{aligned} J_s &= -t^2\left(\frac{2}{U_{12}+\varepsilon} - \frac{4}{U_{12}+\varepsilon+\delta U}\right) \\ &= -t^2\left(\frac{2}{U_{12}+\varepsilon} - \frac{4}{U_{12}+\varepsilon}\left(1+\frac{\delta U}{U_{12}+\varepsilon}\right)^{-1}\right). \end{aligned}$$

With Taylor's expansion, we have

$$\left(1+\frac{\delta U}{U_{12}+\varepsilon}\right)^{-1} \approx 1 - \frac{\delta U}{U_{12}+\varepsilon}.$$

Hence,

$$\begin{aligned} J_s &= -t^2\left(\frac{2}{U_{12}+\varepsilon} - \frac{4}{U_{12}+\varepsilon} + \frac{4\delta U}{(U_{12}+\varepsilon)^2} - \dots\right) \\ &\approx -J_t + \frac{4\delta U}{(U_{12}+\varepsilon^2)^2}. \end{aligned}$$

With the leading order error term of the effective coupling strength given by $4\delta U/(U_{12}+\varepsilon)^2$, the leading error term of the zenith angle in bloch sphere is then given by $4\delta U\tau/(U_{12}+\varepsilon)^2$. Hence, for sufficiently large $U_{12}+\varepsilon$, the error in the tuning of the quantum dots potential can be minimised.

[1] Z. Shi, C. B. Simmons, J. R. Prance, J. K. Gamble, T. S. Koh, Y.-P. Shim, X. Hu, D. E. Savage, M. G. Lagally, M. A. Eriksson, M. Friesen, and S. N. Coppersmith, Phys. Rev. Lett. **108**, 140503 (2012).

[2] C. Gros, R. Joynt, and T. M. Rice, Phys. Rev. B **36**, 381 (1987).